5A90铝锂合金T形接头激光填丝焊接头组织性能分析

何恩光[1]， 巩水利[1]， 杨 涛[2]， 陈 俐[1]

(1. 北京航空制造工程研究所 高能束流加工技术重点实验室，北京 100024;
2. 武汉理工大学 材料科学与工程学院，武汉 430070)

何恩光

摘 要：对2.5 mm厚5A90铝锂合金T形接头激光焊和激光填丝焊接头组织与性能进行了研究. 结果表明，与不填丝相比，焊接过程中填充焊丝有效减少角焊缝咬边、下塌等缺陷，明显改善焊缝表面成形，同时增大了接头熔化区面积，提高了激光的吸收率；填丝还使得T形接头两侧角焊缝组织大小趋于相同，但组织相对粗大；接头抗拉强度接近提高20%，拉伸断口呈韧性断裂.

关键词：T形接头；激光焊；激光填丝焊；5A90铝锂合金；拉伸性能

中图分类号：TG456 **文献标识码**：A **文章编号**：0253－360X(2013)09－0099－04

0 序 言

5A90铝锂合金具有低密度、高比强度、高比刚度、优良的低温性能、良好的耐腐蚀性能和卓越的超塑成形性能，被认为21世纪航空航天工业最理想的轻质高强结构材料. T形接头采用激光填丝焊接方法焊接不但可以保持激光焊熔深大、变形小、精度高等优点，还可以改善激光焊接的焊缝成形，防止裂纹产生，提高接头力学性能等[1,2]. 在对5A90铝锂合金T形接头激光填丝焊接工艺研究的基础上，利用光学显微镜对5A90铝锂合金T形接头激光填丝焊接接头的组织形态进行了分析，测试了接头的拉伸性能，并观察了断口形态.

1 试验方法

激光填丝焊接采用ABB机械手控制的YAG激光填丝焊接系统，包括Trumpf公司的3 kW的HL3006D YAG激光器，Fronius公司的TPS4000 Alu-Edition铝焊专用机/冷送丝复合装置，为了焊接精度，试验还设计了专用的T形接头焊接工装，如图1所示.

试验材料为2.5 mm 5A90铝锂合金轧制板，焊丝为直径1.2 mm的ER5356. 试板尺寸：底板200 mm×300 mm，筋板100 mm×300 mm. 试验采用对T形接头筋板两侧的角焊缝依次进行焊接，焊接过程中利用与激光同轴的喷嘴进行保护，保护气体采用氩气. 为改善导热条件和背部成形，采用开了成形槽的紫铜背衬，并用带孔铜管通氩气进行保护. 焊接过程中激光头中轴线逆着焊接方向偏转8°，且与底板成35°夹角，焊丝沿着焊接方向与底板成60°，激光焦点位于工件上表面.

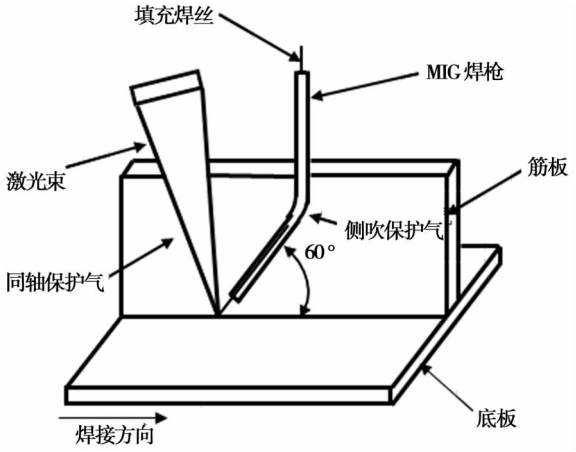

图1 T形接头激光填丝焊装置示意图

Fig. 1 Schematic diagrams of laser filler wire welding device for T-joints

试验后从焊接试板上分别取样进行金相和拉伸试验. 为了解T形接头拉伸性能，采用如图2的试样形式，利用专用夹具完成拉伸性能测试.

收稿日期：2012－12－03

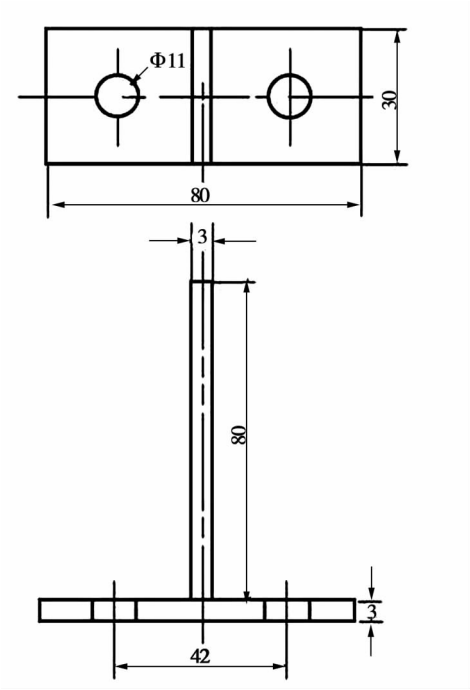

图 2 T 形拉伸试样尺寸(mm)

Fig. 2 Tensile specimen size for T-joints

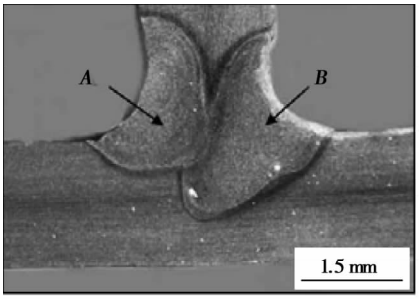

(a) T形接头宏观剖面

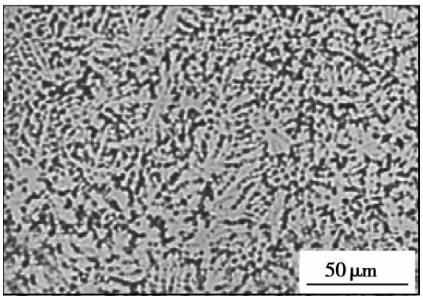

(b) A 侧角焊缝中心组织

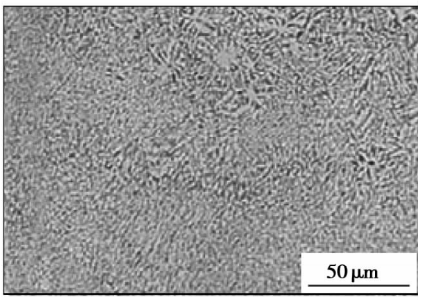

(c) B 侧角焊缝中心组织

图 3 5A90T 形接头激光焊接接头组织

Fig. 3 Microstructure of laser welded 5A90 Aluminum-lithium alloy T-joints

2 结果与讨论

2.1 T 形接头的宏观形貌与组织形态

图 3 和图 4 分别为 5A90 铝锂合金 T 形接头激光焊和激光填丝焊的组织形貌. 图 3a,图 4a 的 T 形接头宏观剖面可以看出,激光焊的 T 形接头两侧角焊缝向筋板侧凹陷比较明显,降低了焊缝的有效承载面积;而填充焊丝的激光焊 T 形接头很好的克服了角焊缝下塌缺陷,焊缝比较饱满,有利于 T 形接头拉伸性能的提高.

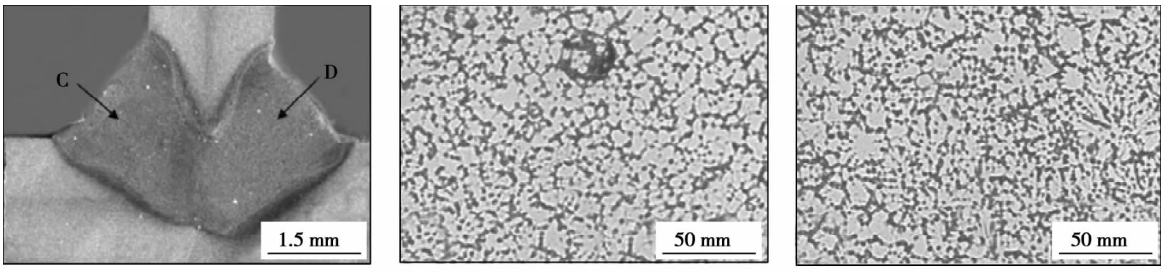

(a) T形接头宏观剖面 (b) C侧角焊缝中心组织 (c) D侧角焊缝中心组织

图 4 5A90T 形接头激光填丝焊接接头组织

Fig. 4 Microstructure of 5A90 aluminum-lithium alloy welded T-joints with laser filler

在对 T 形接头的两侧角焊缝进行依次焊接时,一侧焊缝施焊时的热源对另一侧焊缝都会有影响,再加上角焊缝熔池冷却速率与热传递方向的特殊性,从而使得 T 形接头的熔合区和热影响区变得更加复杂. 在优化的工艺条件下,填充的焊丝在激光直接照射和金属蒸汽等离子体的共同作用下,充分熔化并以熔滴颗粒过渡的方式进入熔池. 熔池随着

热源的远离,以大的冷却速度迅速凝固成焊缝. 熔合区和热影响区在激光热源的作用下,也会发生不同的组织变化. 焊接熔池的凝固决定了焊缝金属的晶体结构、组织和性能. 同时,角焊缝熔池各个方向冷却速度的不同还会造成焊缝组织以及化学成分的不均匀,甚至产生焊接缺陷. 因此分析焊接过程中的熔池凝固具有重要意义.

显微组织观察发现,T 形接头两个角焊缝大致可分为 6 个不同的区域,每一侧角焊缝都是由熔合区、热影响区和母材组成. 其中,熔合区由等轴晶区、柱状晶区和快速冷却区组成; 热影响区由部分熔化区和过热区组成(图 5) . 进一步显微组织观察发现,在筋板一侧,焊缝中的柱状晶生长方向大致与筋板平行,且均匀分布; 而在底板一侧,柱状晶生长方向基本上与底板垂直,沿熔合线由母材向焊缝呈发射状分布. 激光焊的焊缝中心有柱状晶相对生长而产生的交界面; 而激光填丝焊则没有明显的交界面产生,推测可能是焊缝熔滴落入熔池的冲击力加剧了熔池的对流与搅拌,改变了两侧柱状晶的定向生长,进而可以消除柱状晶交界面的产生[3].

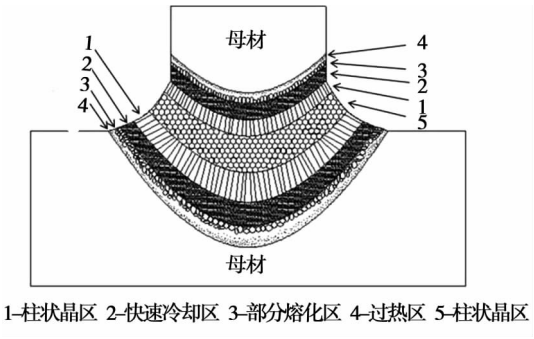

图 5　T 形接头焊缝组织区域示意图

Fig. 5　Schematic diagrams of microstructure areas for weld T-jonts

激光焊和激光填丝焊的焊缝热影响区均不明显,部分熔化区较小,熔合区组织大部分为柱状晶. 这是因为熔池中低沸点元素(如 Mg 等) 的蒸发烧损,使熔池固液界面前沿的液相中成分过冷度增大,晶粒依附于热影响区局部熔化的母材界面,直接从熔池壁上形核结晶,并逆着最大热梯度方向生长,即与母材晶粒联生结晶,外延长大[5-8]. 晶粒从焊缝边界联生结晶后,垂直于熔合线以柱状晶的形式向熔池中心生长. 随着熔池中热梯度方向的改变,晶粒生长方向也发生改变,导致联生结晶被抑制,柱状晶转化为等轴枝晶.

T 形接头焊接时,由于两侧角焊缝是依次进行焊接的,因此后施焊的热源对先施焊的焊缝组织会产生较大影响. 激光焊 T 形接头两侧角焊缝中心的组织差异较大,先施焊的 A 侧角焊缝中心组织(图 5b) 明显比后施焊的 B 侧焊缝中心组织(图 5c) 粗大. 这是由于在对 B 侧进行焊接时,激光热源相当于对 A 侧焊缝组织进行了热处理,从而使其组织变的相对粗大. 而激光填丝焊时,先焊的 C 侧焊缝中心组织(图 3b) 与后焊的 D 侧焊缝中心组织(图 3c) 差别不大,但是晶粒相对于激光时较为粗大,且组织大小也较为均匀. 可以推测填充焊丝可以增加材料对激光的吸收率,致使熔池冷却速率下降,焊缝组织相对粗大. 同时,焊丝熔滴向熔池过渡时的搅拌和对流使焊缝组织变得更加均匀.

综上所述,T 形接头激光填丝使两侧角焊缝组织趋于均匀,同时填充焊丝弥补了焊接过程中的母材金属的损失,显著改善了角焊缝表面成形.

2.2　焊接接头的拉伸性能及断口特征

激光焊和激光填丝焊 T 形接头拉伸强度的计算公式为: $\sigma = F_N/S$,式中 F_N 是拉伸过程的最大载荷; S 为承受载荷的最小面积,为了便于计算,等效为筋板横截面面积. 激光焊焊接接头的抗拉强度达到母材抗拉强度的 70.6%,激光填丝焊则达到了母材抗拉强度的 87.1%.

观察 T 形拉伸的拉断试样发现: 激光焊试样的断裂全部发生在焊缝中心或热影响区. 出现这种现象的主要原因是,激光焊接接头中柱状晶相对生长的交界面使焊缝中心成为接头的薄弱区; 同时,激光焊的焊缝织表面常有咬边、表面凹陷及表面不平滑等宏观缺陷,造成横截面面积减小进而承载能力下降,抗拉强度降低.

激光填丝焊接接头的抗拉强度有明显的改善,拉伸试样断裂主要发生在靠近筋板侧的焊缝或热影响区. 其接头的抗拉强度比激光焊接头抗拉强度提高 20% 左右,说明激光填丝焊接接头具有更好的拉伸性能. 因为填充焊丝的加入不仅消除了焊缝中心柱状晶交界面的薄弱区,还使得两侧角焊缝组织更加均匀,而且角焊缝有效承载面积增大,以及强元素 Mg 含量的补充,这些都为抗拉强度的提高做了贡献.

图 6 为室温拉伸断口形貌,从图 6a 可以看出,激光焊接头断裂发生在热影响区的断口主要由粗大的穿晶解理平面组成,晶粒较大,韧窝较少; 从图 6b 可见,母材的断口呈颗粒状断面,颗粒间有塑性拉伸的痕迹; 从图 6c 可知,激光填丝焊接头的断口上有大量韧窝,大韧窝内部有小韧窝,大韧窝之间也有小韧窝分布.

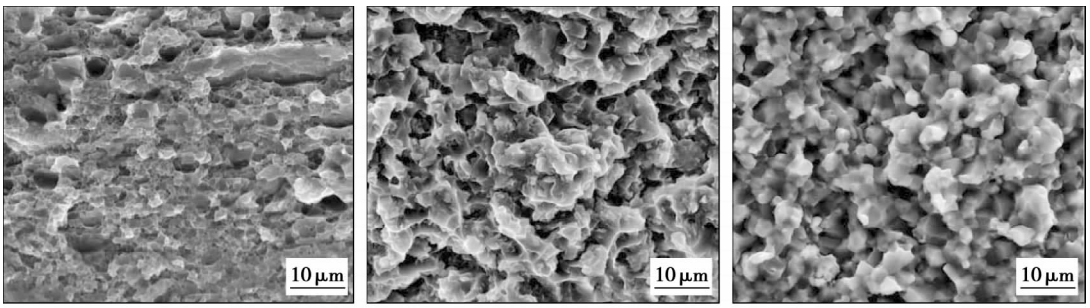

(a) 激光焊
(热影响区断口)

(b) 激光填丝焊
(母材断口)

(c) 激光填丝焊
(热影响区断口)

图 6 激光焊及激光填丝焊拉伸试样断口扫描形貌

Fig. 6 Scan photos of tensile specimen fracture for laser welding and laser filler wire welding

3 结 论

(1) T 形接头激光焊接过程中,填充焊丝可以改善材料对激光的吸收率,增加焊缝熔宽,改善角焊缝成形,还可以使得 T 形接头两侧角焊缝组织均匀一致,但会造成显微组织的相对粗大.

(2) 在优化工艺条件下,激光焊焊接接头 T 形拉伸抗拉强度达到了母材的 70% 以上; 相对于激光焊,而激光填丝焊可以显著提高 T 形接头的拉伸性能,接头抗拉强度接近提高 20%.

(3) 激光焊接接头热影响区断口由粗大的穿晶解理平面组成; 而采用 ER5356 焊丝的激光填丝焊焊接接头的断口呈韧窝形貌.

参考文献:

[1] 任家烈, 吴爱萍. 先进材料的连接 [M]. 北京: 机械工业出版社, 2000.

[2] 刘会杰. 焊接冶金与焊接性 [M]. 北京: 机械工业出版社, 2007.

[3] Gerritsen C H J. Hybrid Nd: YAG laser MAG welding of T joints in C-Mn steels for shipbuilding application [R]. United Kingdom: The Welding Instiute, 2004: 1 - 40.

[4] Squillade A, Prisco U. Influence of filler material on micro-and macro-mechanical behavior of laser-beam-welded T-joint for aerospace applications [J]. Journal Materials: Design and Applications, 2009(223): 103 - 115.

[5] Chen Yanbin, Li Liqun, Peng Xiaoyun, *et al*. Joints performance in laser welding Al alloy with filler wire [J]. Transactions of the Nonferrous Metals Society of China. 2005, 15(2): 87 - 91.

[6] 崔 丽, 李晓延, 巩水利, 等. 5A90 铝锂合金激光焊接焊缝微观组织特征 [J]. 焊接学报, 2010, 31(9): 77 - 84.
Cui Li, Li Xiaoyan, Gong Shuili, *et al*. Microstructure investigation of Nd: YAG laser welded 5A90 aluminium-litium alloys [J]. Transactions of the China Welding Institution, 2010, 31(9): 77 - 84.

[7] 祁俊峰, 丁 鹏, 张冬云, 等. 工艺参数对铝合金 CO_2 激光焊接光致等离子体温度的影响 [J]. 焊接学报, 2008, 29(6): 97 - 100.
Qi Junfeng, Ding Peng, Zhang Dongyun, *et al*. Influence of welding parameters on laser-induced plasma temperature in CO_2 laser welding of aluminum alloys [J]. Transactions of the China welding Institution, 2008, 29(6): 97 - 100.

[8] 陈 铠, 肖荣诗, 张盛海, 等. 高强铝合金激光粉末焊接过程 [J]. 焊接学报, 2006, 27(10): 33 - 36.
Chen Kai, Xiao Rongshi, Zhang Shenghai, *et al*. CO_2 laser welding process of aluminum alloy with filler power [J]. Transactions of the China welding Institution, 2006, 27(10): 33 - 36.

作者简介: 何恩光,男,1984 年 10 月出生,助理工程师. 主要研究方向为铝合金激光焊接. Email: enguanghe@qq.com

ing; intermetallic compound

Design and characteristics analysis of spot welding servo pressure device LI Haibo, CAO Biao (School of Mechanical and Automotive Engineering, South China University of Technology, Guangzhou 510640, China). pp 91 – 94

Abstract: A spot welding servo pressure device was designed to solve the fluctuation and non-control of pressure during spot welding process with pneumatic welding gun. The developed device had the advantages of soft contact between the electrodes and workpiece, quickly imposing pressure and accurate pressure control. Dynamic analysis was carried out on the designed servo pressure device, and a transfer function model based on the control mode and equivalent reference model based on the dominant pole were established. The relationship between the mechanical parameters of the servo pressure device and its damping ratio and natural oscillation frequency was acquired, and the influence of mechanical parameters on the system stability and dynamic characteristics was also analyzed.

Key words: resistance spot welding; servo pressure; dynamic characteristic

Three-dimensional numerical modeling of influences of process parameters on arc fluctuation in plasma arc torch

YE Xiangyi, ZHENG Zhenhuan, LI Qiang (School of Materials Science and Engineering, Fuzhou University, Fuzhou 350108, China). pp 95 – 98

Abstract: A three-dimensional transient turbulent model of plasma arc was established based on local thermodynamic equilibrium (LTE) to study the effects of arc current, argon flow rate and hydrogen flow rate on arc fluctuation inside the argon-hydrogen plasma torch by using computational fluid dynamics software ANSYS CFX. The results show that when the arc current increased but less than 600 A, the arc column became shorter, the average arc voltage and the arc fluctuation decreased, but the fluctuation frequency increased. However, when the arc current increased to above 600 A, it had little influence on the arc fluctuation. The increase of argon flow rate or hydrogen flow rate led to the increase of the arc column, average arc voltage and voltage fluctuation, but decrease of the fluctuation frequency. Among three process parameters, hydrogen flow rate affected the arc fluctuation most, and the arc current did least.

Key words: plasma spraying; three-dimensional simulation; transient modeling; arc fluctuation; process parameters

Microstructure and properties of 5A90 Al-Li alloy T-joints by laser welding with filler wire HE Enguang[1], GONG Shuili[1], YANG Tao[2], CHEN Li[1] (1. Key Laboratory of High Energy Density Beam Processing Technology, Beijing Aeronautical Manufacturing Technology Research Institute, Beijing 100024, China; 2. School of Material Science and Engineering, Wuhan University of Science and Technology, Wuhan 430070, China). pp 99 – 102

Abstract: The microstructure and mechanical properties of 5A90 Al-Li alloy T-joints by laser welding with and without filler wire were investigated. The results show that laser welding with filler wire could reduce the undercut and collapse defects, and improve the weld surface forming. Meanwhile, laser welding with filler wire could also increase the area of fusion zone and enhance the laser absorption rate. Laser welding with filler wire could homogenize the weld microstructure on both sides of the T-joint, although the grains were coarsened. However, the tensile strength of the joint increased by nearly 20% and the fractured surface revealed ductile features.

Key words: T-joint; laser welding; laser welding with filler wire; 5A90 Al-Li alloy; tensile property

Influence of geometrical parameters on specific strength of Ti-based alloy honeycomb unit JING Yongjuan[1], LI Xiaohong[1], XIE Zonghong[2], YUE Xishan[1] (1. Beijing Aeronautical Manufacturing Technology Research Institute, Beijing 100024, China; 2. School of Astronautics, Northwestern Polytechnical University, Xi´an 710000, China). pp 103 – 106

Abstract: The influence of the geometrical parameters, the inscribed circle diameter D and the cell wall thickness t, on the density and strength of the honeycomb unit made with Ti-based alloy was investigated. It was found that when D was large and t was thin, the microstructure of the weld interface was discontinuous and differed in grain sizes, which would seriously deteriorate the strength of the honeycomb unit. The unit strength could be expressed as $\sigma = 118.8 \times t_{-3.44}$ when D was 11.2 mm, or $\sigma = 262.8 \times t_{-5.94}$ when D was 6.4 mm. High specific strength was obtained with D as 4.8 mm and t as 0.05 mm. The quantitative relation between the geometrical parameters and specific strength could be estimated by the specific strength of the honeycomb unit with Ti-based alloys.

Key words: Ti-based alloy; honeycomb; geometrical parameter

Progress of methods for decreasing residual thermal stresses in ceramic/metal joints XIONG Huaping, WU Shibiao, CHEN Bo, MAO Wei (Laboratory of Welding and Forging, Beijing Institute of Aeronautical Materials, Beijing 100095, China). pp 107 – 112

Abstract: Large residual thermal stress is usually formed within ceramic/metal joints because of the great mismatch in thermo-physical properties between the ceramic and metal to be joined. How to decrease the residual thermal stresses within the ceramic/metal joints has been always an important research branch in the field of ceramic (or ceramic matrix composite) joining. Seven methods for decreasing residual thermal stresses are summarized based on the worldwide research results in decades, in which the conceptions of buffer layer, gradient and composite are very important, and their mechanisms are analyzed. In order to achieve better effect, the authors suggest that different methods for decreasing residual thermal stresses should be combined with each other, and it would be an interesting research area.

Key words: ceramic/metal; thermal expansion coefficient; residual thermal stress; buffer layer; composite; gradient